Mutations in *SLC33A1* Cause a Lethal Autosomal-Recessive Disorder with Congenital Cataracts, Hearing Loss, and Low Serum Copper and Ceruloplasmin

Peter Huppke,[1,14,*] Cornelia Brendel,[1,14] Vera Kalscheuer,[2] Georg Christoph Korenke,[3] Iris Marquardt,[3] Peter Freisinger,[4] John Christodoulou,[5] Merle Hillebrand,[1] Gaele Pitelet,[6] Callum Wilson,[7] Ursula Gruber-Sedlmayr,[8] Reinhard Ullmann,[2] Stefan Haas,[9] Orly Elpeleg,[10] Gudrun Nürnberg,[11] Peter Nürnberg,[11] Shzeena Dad,[12] Lisbeth Birk Møller,[12] Stephen G. Kaler,[13] and Jutta Gärtner[1]

Low copper and ceruloplasmin in serum are the diagnostic hallmarks for Menkes disease, Wilson disease, and aceruloplasminemia. We report on five patients from four unrelated families with these biochemical findings who presented with a lethal autosomal-recessive syndrome of congenital cataracts, hearing loss, and severe developmental delay. Cerebral MRI showed pronounced cerebellar hypoplasia and hypomyelination. Homozygosity mapping was performed and displayed a region of commonality among three families at chromosome 3q25. Deep sequencing and conventional sequencing disclosed homozygous or compound heterozygous mutations for all affected subjects in *SLC33A1* encoding a highly conserved acetylCoA transporter (AT-1) required for acetylation of multiple gangliosides and glycoproteins. The mutations were found to cause reduced or absent AT-1 expression and abnormal intracellular localization of the protein. We also showed that AT-1 knockdown in HepG2 cells leads to reduced ceruloplasmin secretion, indicating that the low copper in serum is due to reduced ceruloplasmin levels and is not a sign of copper deficiency. The severity of the phenotype implies an essential role of AT-1 in proper posttranslational modification of numerous proteins, without which normal lens and brain development is interrupted. Furthermore, AT-1 defects are a new and important differential diagnosis in patients with low copper and ceruloplasmin in serum.

Introduction

Copper is an essential metal that facilitates electron transfer reactions and is incorporated in many cuproenzymes that are involved in mitochondrial respiration, antioxidant defense, connective tissue formation, neurotransmitter and melanin biosynthesis, and peptide amidation.[1] Excess amounts of copper, however, are toxic because they facilitate the production of reactive oxygen species. Because of a tightly controlled copper homeostasis, intracellular free copper is limited to less than one free copper ion per cell.[2] After absorption in the duodenum, copper is rapidly removed from the portal circulation by the liver, the central organ in copper homeostasis, where it is incorporated in cuproenzymes, distributed to the general circulation, or secreted into bile (the major mechanism for copper elimination).[1]

The human disorders of copper metabolism with a known molecular defect are Wilson disease (MIM 277900), Menkes disease (MIM 309400), and aceruloplasminemia (MIM 604290).[3–5] In all of them, low serum copper and ceruloplasmin are the diagnostic hallmarks. However, only one disorder, Menkes disease, is caused by copper deficiency. Defects of ATP7A, a Cu^{1+}-transporting ATPase expressed in extrahepatic tissues, lead to excessive intestinal copper accumulation and severe systemic copper deficiency.[6–8] In Wilson disease and aceruloplasminemia, body copper levels are not reduced; on the contrary, in Wilson disease they are increased because of reduced excretion of copper in the bile. In these disorders the low copper in plasma is a result of low or absent ceruloplasmin, the carrier of 95% of the plasma copper.

In 2005, Horvath et al. described a patient with low serum copper and ceruloplasmin with a phenotype unlike Wilson and Menkes disease or aceruloplasminemia.[9] The syndrome was considered to represent a possible novel defect in human copper metabolism, and several known copper transport genes were evaluated and excluded as underlying causes. We encountered four additional patients from three other families with a clinical and

[1]Department of Pediatrics and Pediatric Neurology, Georg August University, 37075 Göttingen, Germany; [2]Department of Human Molecular Genetics, Max Planck Institute for Molecular Genetics, 14195 Berlin, Germany; [3]Department of Neuropediatrics, Children's Hospital, 26133 Oldenburg, Germany; [4]Department of Pediatrics, Klinikum am Steinenberg, 72764 Reutlingen, Germany; [5]Western Sydney Genetics Program, The Children's Hospital at Westmead, and Disciplines of Paediatrics and Child Health and Genetic Medicine, Sydney Medical School, University of Sydney, 2145 Westmead, Australia; [6]Service de Neuropédiatrie, CHU Nice, 6200 Nice, France; [7]National Metabolic Service, Starship Children's Hospital, 1142 Auckland, New Zealand; [8]Department of Pediatrics, Medical University of Graz, 8010 Graz, Austria; [9]Department of Computational Molecular Biology, Max Planck Institute for Molecular Genetics, 14195 Berlin, Germany; [10]Monique and Jacques Roboh Department of Genetic Research, Department of Genetic and Metabolic Diseases, Hadassah, Hebrew University Medical Center, 91050 Jerusalem, Israel; [11]Cologne Center for Genomics, Center for Molecular Medicine Cologne (CMMC), and Cologne Excellence Cluster on Cellular Stress Responses in Aging-Associated Diseases (CECAD), University of Cologne, 50931 Cologne, Germany; [12]Department for Applied Human Molecular Genetics Kennedy Center, 2600 Glostrup, Denmark; [13]Unit on Human Copper Metabolism, Molecular Medicine Program, The Eunice Kennedy Shriver National Institute of Child Health and Human Development, National Institutes of Health, Bethesda, MD 20814, USA
[14]These authors contributed equally to this work
*Correspondence: phuppke@med.uni-goettingen.de
DOI 10.1016/j.ajhg.2011.11.030. ©2012 by The American Society of Human Genetics. All rights reserved.

biochemical phenotype closely similar to that reported by Horvath et al. We sought to identify the primary genetic defect for this unique clinical and biochemical disease entity.

Subjects and Methods

Five patients from four families were included in the study. All legal representatives gave written informed consent to the study and the study was approved by the local institutional review boards. Clinical features of patient 4 have already been published.[9]

Homozygosity Mapping

Genome-wide linkage analysis was performed with the Affymetrix GeneChip Human Mapping 250K Nsp Array. Data handling, evaluation, and statistical analysis was performed as described previously.[10]

Deep Sequencing

Prior to deep sequencing, patient DNAs from the homozygous interval were enriched by means of a Sure Select Capture Array according to the manufacturer's protocols (Agilent, Santa Clara, CA). The custom-designed array comprised 242,393 probes representing 1,623 exons mapping to the genomic interval chr3: 153423761–166861604, hg19 with a 3 bp tiling and a 69 bp extension on each side. Repetitive sequences were not masked.

Single-end deep sequencing was performed on the Solexa Genome Analyzer GAIIx. Read length was 76 nt. Sequences were analyzed with in-house-developed tools.

Mutation Analysis by Sanger Sequencing

Total genomic DNA was prepared from peripheral blood samples according to standard procedures.[11] The six exons including intron-exon boundaries of *SLC33A1* (Genbank accession NG_023365.1) were analyzed by direct sequencing on an ABI 377 semiautomated sequencer via the DNA Dye Terminator Cycle Sequencing Kit (Applied Biosystems, Darmstadt, Germany) according to the manufacturer's instructions.

Construction of Eukaryotic Expression Vectors

Expression vectors, encoding wild-type human *SLC33A1* and mutated *SLC33A1*, were constructed as follows. Full-length wild-type *SLC33A1* cDNA was amplified via PCR with cDNA generated from wild-type human fibroblasts and oligonucleotides containing restriction enzyme sites (*SLC33A1* cDNAFLAG forward, 5′-atagtcgacatgtcacccaccatctccc-3′; *SLC33A1* cDNAFLAG rev, 5′-ataggatccttaattgttccttttgcatttcc-3′; *SLC33A1* cDNA-EGFP-N1 forward, 5′-atactcgagatgtcacccaccatctccc-3′; *SLC33A1* cDNA-EGFP-N1 rev, 5′-ataggatccaaattgttccttttgcatttcc-3′). *SLC33A1* mutants were generated by site-directed mutagenesis PCR with the vector containing wild-type *SLC33A1* cDNA as template (*SLC33A1* 328G>C forward, 5′-gctatacagaccaaccttttcttcagttttg-3′; *SLC33A1* 328G>C rev, 5′-caaaactgaagaaaggttggtctgtatagc-3′; *SLC33A1* 1098C>G forward, 5′-gattatcagcaaatagactgcaggtccccag-3′; *SLC33A1* 1098C>G reverse, 5′-ctggggacctgcagtctatttgctgataatc-3′). Synthesized wild-type and mutant cDNAs were cloned into the eukaryotic expression vector p3xFLAG-CMV 7.1 (Sigma-Aldrich Chemie GmbH, Steinheim, Germany) pEGFP-N1 (Clontech Laboratories, Inc., Mountain View, CA, USA). All constructs were verified by Sanger sequencing.

Antibodies

Commercially available antibodies were used for the detection of Protein Disulfide Isomerase (PDI; rabbit polyclonal antibody; Sigma-Aldrich Chemie GmbH), Giantin (rabbit polyclonal antibody; Covance, Emeryville, CA, USA), Syntaxin 6 (rabbit monoclonal antibody [C34B2]; Cell Signaling Technology, Danvers, MA, USA), Ceruloplasmin (mouse monoclonal [3B11]; Abcam, Cambridge, UK), Albumin (mouse monoclonal anti-human Albumin Clone HSA-11, Sigma, Saint Louis, MO, USA), and GAPDH (mouse monoclonal [6C5] to GAPDH; Abcam). Recombinant proteins were detected with mouse monoclonal anti-FLAG M2 antibody (for western blot: Stratagene GmbH, La Jolla, CA, USA; for immunofluorescence: SIGMA-Aldrich, Taufkirchen, Germany) or mouse monoclonal anti-GFP antibody (JL9, Cell Signaling Technology). As secondary antibodies for immunofluorescent staining, goat anti-mouse IgG Cy3 and anti-rabbit IgG Cy3 (Jackson Immuno-Research Laboratories, West Grove, PA, USA) and Alexa Fluor 488 goat anti-rabbit IgG and anti-mouse IgG (Molecular Probes Inc., Eugene, OR, USA) were used.

Minigene Construct

Genomic DNA fragments containing *SLC33A1* wild-type (c.1267−1G) and mutant (c.1267−1A) exon 5 along with 260 bp of 5′ and 274 bp of 3′ intronic flanking sequences, were amplified by PCR and cloned into the EcoRI and BamHI sites of the exon trapping vector pSPL3 (GIBCO BRL). After the verification of the minigene constructs by sequencing, HeLa cells were transiently transfected each with both constructs. After 24 hr, total RNA was extracted, reverse transcribed, amplified, and sequenced. Oligonucleotides used for minigene construction, amplification, and sequencing are listed in Table S1 available online.

Quantitative Real-Time PCR

First-strand cDNAs for qRT-PCR of RNA generated from patient and control fibroblasts were synthesized as described above. Quantitative RT-PCR was performed with the iQ5 cycler (BioRad Laboratories) and the iQ SYBR Green Supermix kit (BioRad Laboratories). All qRT-PCR reactions were performed in triplicate. Annealing temperatures for the genes were set to 57°C. Primer sequences (*GAPDH, SLC33A1*) are listed in Table S1. Reaction specificity was controlled by postamplification melting curve analysis. Relative expression rates of target gene transcripts were calculated with the $2^{-(\Delta\Delta Ct)}$.

Results

Five patients were included in the study. Four were from consanguineous families. Patients 1 and 2 were siblings originating from Tunisia, patient 3 was from Turkey, patient 4 was from Saudi Arabia, and patient 5 was from New Zealand. A summary of the genetic, laboratory, and clinical data is given in Table 1 and the family pedigrees are presented in Figure 1. All five patients presented with a complex but similar phenotype. Severe psychomotor retardation was present in all of them. None of the patients was able to sit or walk independently and none learned to speak. Less frequent were nystagmus (n = 3) and seizures (n = 2). All patients died prematurely between ages 22 months and 6 years. Causes of death included pneumonia (n = 2), kidney failure (n = 1), and multiorgan

Table 1. Phenotype and Genotype of the Patients with *SLC33A1* Mutations

Patient	1	2	3	4	5
Sex	M	F	M	M	M
Parental consanguinity	yes	yes	yes	yes	no
Ancestry	Tunisia	Tunisia	Turkey	Saudi Arabia	New Zealand
Mutation: DNA level	c.1267−1G>A	c.1267−1G>A	c.1098C>G	c.328G>C	c.615_616insT, c.1474_c.1482+9del
Mutation: protein level			p.Tyr366*	p.Ala110Pro	p.Leu205Phefs*31
Ceruloplasmin in plasma mg/l (200–600)	nd	<50	20–30	91–95	<20
Copper in plasma μg/dl (70–150)	nd	17.5	<10	36–68	19
64Cu uptake in fibroblasts (8.2–30.8 ng)	nd	nd	56.7	41.3	54.8
Age at death (months)	72	22	42	48	22
Congenital cataracts	+	+	+	+	+
Nystagmus	+	-	+	+	-
Hearing loss	+	+	+	+	+
Developmental delay	+	+	+	+	+
Cerebellar atrophy	+	+	+	+	+
Cerebral atrophy	+	+	+	+	+
Hypomyelination	+	+	+	+	+

Normal values for copper and ceruloplasmin are given in brackets. Abbreviations: nd, not done; M, male; F, female.

failure (n = 1). In one case the cause of death is unknown. Magnetic resonance imaging (MRI) of the brain showed a uniform pattern with cerebellar hypoplasia, wide subarachnoid spaces, and hypomyelination (Figure 2). Serum copper was low (10%–20% of the low normal rage) and ceruloplasmin very low or undetectable in four patients. In patient 1, brother of patient 2, biochemical evaluation was not done and the patient died before the diagnosis was made. Copper levels in urine were normal (n = 3), as were levels in CSF (n = 2) and in liver (n = 1). Three patients were treated with copper orally or subcutaneously. In the patient described by Horvath et al.,[9] copper treatment was reported to have had beneficial effects but he nevertheless died at age 4 years. In all three of the treated subjects, serum copper and ceruloplasmin levels remained low.

By using the SNP array genotype data of four patients (patients 1, 2, 3, and 4) from three consanguineous families, we observed a single significant genome-wide linkage peak on chromosome 3q25 with a maximum multipoint LOD score of 4.51 (Figure S1). The underlying common homozygous region between the SNP markers rs9823065 and rs7646008 defined a candidate region of 13.4 Mb (neucleotides 153423761–166861604, hg19). Array-based sequence capture of this region, followed by next-generation sequencing in patients 2 and 4, showed two homozygous mutations affecting the same gene, *SLC33A1*, coding for the membrane acetyl-CoA transporter (AT-1).[12] A mutation search in the *SLC33A1* gene performed in the remaining patients by conventional Sanger sequencing showed mutations in all (Figure 3). In patients 1 and 2, siblings from a consanguineous Tunisian family, a homozygous mutation of the acceptor splice site of exon 5, c.1267−1G>A, leading to partial or complete loss of exon 5 was identified (Figure S2). In patient 3, a boy from a consanguineous Turkish family, a homozygous nonsense mutation c.1098C>G (p.Tyr366*) was detected that causes a premature stop after 366 amino acids (Figure S3). In patient 4, described earlier by Horvath et al.,[9] sequencing of the *SLC33A1* gene revealed a homozygous missense mutation c.328G>C (p.Ala110Pro) that was not present in 122 unrelated control individuals. The mutation introduces a proline instead of the highly conserved alanine at position 110 of the polypeptide (Figure S4). Topological prediction of mutant AT-1 with the SOSUI program predicts that the mutation causes a structural change in the first and second transmembrane domain. The fifth patient, the only child in the cohort from a nonconsanguineous family, was found to be compound heterozygous for the c.615_616insT mutation (p.Leu205Phefs*31) leading to a frame shift with a premature stop codon after 31 amino acids and the deletion c.1474_c.1482+9del leading to the loss of three amino acid residues and 9 bp in intron 5 including the donor splice site. DNA from the parents of patients 3 and 5 was available and showed that they were heterozygous for the mutations (Figure S3).

To assess the functional consequences of the mutations, we performed quantitative real-time PCR in fibroblasts from patients 3, 4, and 5 (Figure 4). Compared to normal

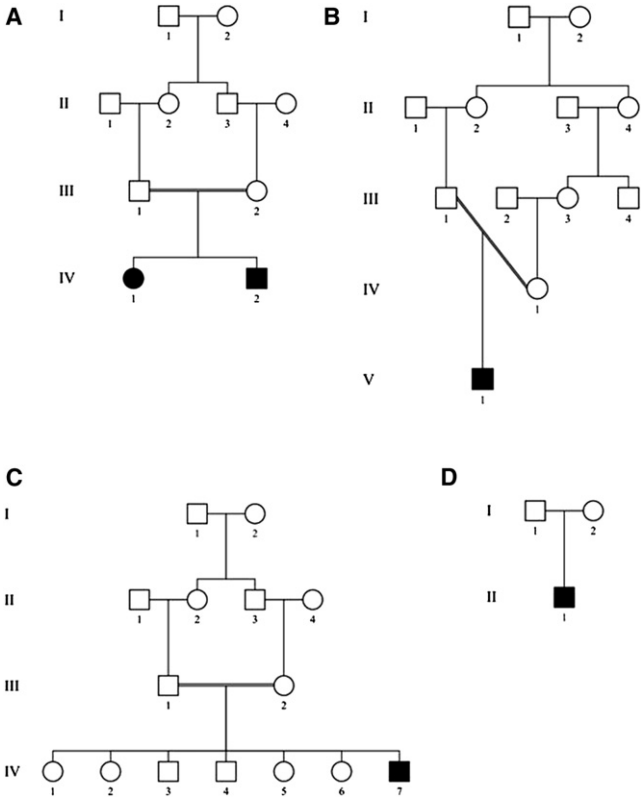

Figure 1. Family Pedigrees
(A) Patients 1 and 2; (B) patient 3; (C) patient 4; (D) patient 5.

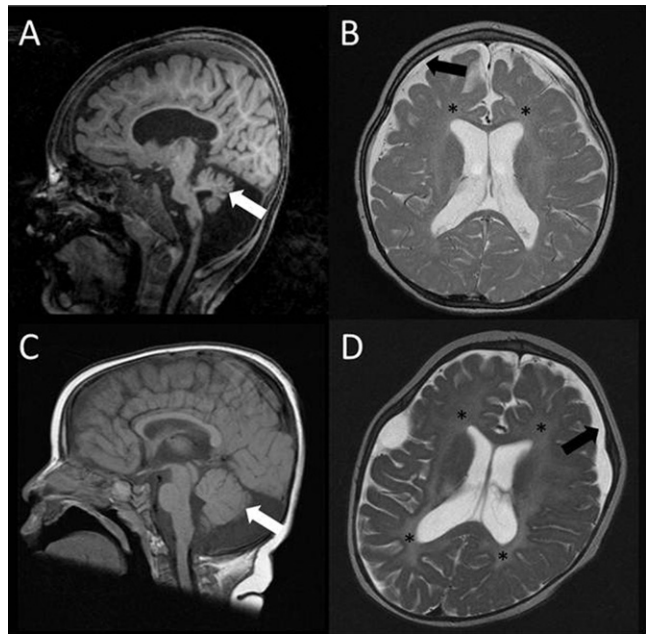

Figure 2. Cranial MRI Images
Patient 3 at age 36 months (A, B) and patient 5 at age 14 months (C, D). Sagittal T1 images (A, C) demonstrate cerebellar hypoplasia (white arrows); transversal T2 images (B, D) show wide subarachnoid spaces (black arrows) and hypomyelination (*).

control cells, the relative expression of *SLC33A1* remains unaltered by the missense mutation p.Ala110Pro whereas the *SLC33A1* mRNA level decreased 20% in fibroblasts of patient 5 carrying a compound heterozygous mutation. As a result of the nonsense mutation p.Tyr366*, we observed a significantly reduced relative expression of *SLC33A1* in fibroblasts of patient 3, most probably because of the quality-control function nonsense-mediated mRNA decay.

Next we investigated the intracellular localization and protein expression of endogenous AT-1 in patient fibroblasts by using immunocytochemical staining and western blot analysis. After unsuccessful experiments with commercially available AT-1-specific antibodies (data not shown), we generated different vectors expressing N terminally FLAG-tagged AT-1 fusion proteins. Western blot analysis of lysates from transiently transfected MCF-7 cells showed that the expressed fusion proteins FLAG-AT-1 wild-type and FLAG-AT-1 p.Ala110Pro were detected at the expected size of 62 kDa. In lysates of cells transiently transfected with the construct carrying the p.Tyr366* mutation, the full-length protein is missing but we detected a shortened protein of around 43 kDa.

The above described expression vectors were then used to analyze the intracellular localization of AT-1 in MCF-7 (Figure 4), HeLa, and CHO (data not shown). Contrary to previous work, where AT-1 was described as restricted to the ER membrane, immunocytochemistry with a specific FLAG antibody showed that the wild-type AT-1 protein displayed a perinuclear cytoplasmic distribution and colocalizes with marker proteins of the *cis*-, *medial*-, and *trans*-Golgi. To exclude that the localization was a specific effect of the FLAG-tag, we repeated the experiment with a GFP-tag but obtained a similar result (Figure S5). The missense mutation p.Ala110Pro produced a punctate staining pattern in the cytoplasm that failed to colocalize with the Golgi marker, and the nonsense mutant protein p.Tyr366* was found to be distributed in the cytoplasm where it strongly colocalized with the ER marker protein PDI (Figure 4).

An intriguing finding in all the patients described in this article was that copper and ceruloplasmin levels in serum were very low. To analyze whether there is a direct association between AT-1 expression and hepatic ceruloplasmin secretion, we reduced AT-1 expression in HepG2 cells by using small interfering RNA (siRNA) (Figure 5). As a result of this treatment, we observed not only decreased *SLC33A1* mRNA levels 2 days after siRNA transfection but also a 30% reduced secretion of ceruloplasmin in the medium of treated HepG2 cells compared to controls. These results indicate that AT-1 expression and ceruloplasmin secretion are indeed connected. To exclude that the reduction of ceruloplasmin secretion is a nonspecific sign of reduced protein synthesis, we analyzed the secretion of a second protein, albumin, after siRNA knockdown and found that it was unaltered (Figure 5).

Figure 3. Genomic Structure and Localization of the Mutations in the *SLC33A1* Gene
The coding region is depicted in gray. Missense mutation, arrow; nonsense mutation, X; splice site mutation, asterisk; insertion, down triangle; deletion, up triangle.

Discussion

In the present study, we describe a novel severe childhood disorder leading to death in early childhood. The phenotype includes congenital cataracts, hearing loss, severe developmental delay, and cerebellar hypoplasia and is associated with low serum copper and ceruloplasmin. Genetic analysis revealed that all patients are either homozygous or compound heterozygous for mutations in the *SLC33A1* gene coding for AT-1, the ER membrane acetyl-CoA transporter. Four of five mutations detected in the *SLC33A1* gene can be expected to severely impair the function of AT-1 by leading to a shortened or absent protein. In patient 4, sequencing revealed a homozygous missense mutation, p.Ala110Pro, in exon 1. Supporting its pathogenicity is the fact that Ala110 is a highly conserved residue in AT-1 and the mutation was not detected in normal controls. Furthermore, topological prediction via the SOSUI program shows that the mutation leads to changes in the first and second transmembrane domains.

In 2008 it was reported that a heterozygous missense mutation in *SLC33A1*, p.Ser113Arg, caused autosomal-dominant spastic paraplegia (SPG42) in a large Chinese family.[13] In a subsequent study, 220 patients with autosomal-dominant spastic paraplegia were screened for mutations in the *SLC33A1* gene but no mutations were detected.[14] There is no obvious overlap between the phenotype reported with p.Ser113Arg AT-1 mutation and the phenotype we delineate here. Moreover, none of the parents of the children described here who were heterozygous for AT-1 mutations showed clinical signs of spastic paraplegia. To date it therefore seems likely that *SLC33A1* is not the SPG42 gene. On the other hand, in previous reports, cataracts and optic atrophy were reported in association with spastic paraplegia.[15–17] *SLC33A1* might be a candidate gene in these cases.

To analyze the functional consequences of the *SLC33A1* mutations detected in this study, we analyzed the subcellular localization of the mutant proteins. The experiments showed a clear difference between the localization of the AT-1 wild-type protein and the mutant proteins. However, our experiments showed a localization of wild-type AT-1 in the *cis*-, *medial*-, and *trans*-Golgi and not in the ER as described previously.[18] Jonas, Pehar, and Puglielli (2010) analyzed the subcellular localization by transfecting AT-1 that contained a Myc-His tag in CHO cells followed by SDS-PAGE and immunoblotting after separation of intracellular membranes on a Nycodenz gradient.[18] To exclude that the FLAG tag we used had influenced the localization, we repeated the experiment with a GFP tag but again found that wild-type AT-1 was located in the Golgi. We also considered that different cell types might display a different localization of AT-1 and repeated the experiments in HeLa and CHO cells. However, the localization was similar in all cell types. Therefore, most probably the conflicting results are due to the different methods used to determine the localization of AT-1. In light of the presumed function, it is important to further clarify the exact subcellular localization.

AT-1 is a multiple transmembrane protein that consists of 549 amino acids and has a mass of 60.9 kDa.[12] AT-1 is reported to be responsible for the transport of acetyl-CoA into the lumen of the ER, serving as a substrate for acetyltransferases. Acetylation is an important reversible post-translational modification of many proteins. In a recent study, lysine acetylation sites were identified on more than 1,700 proteins involved in various crucial cellular processes such as splicing, chromatin remodeling, and nuclear transport.[19] It has been described that AT-1 is essential for the transient acetylation of β-site APP cleaving enzyme I (BACE1). Only acetylated intermediates of BACE1 reach the Golgi complex whereas nonacetylated intermediates are degraded in a post-ER compartment.[20] The current knowledge about AT-1 does not offer an explanation for why mutations in AT-1 lower copper and ceruloplasmin levels. One possible explanation is that ceruloplasmin, as a secreted glycoprotein, requires transient acetylation for proper function and the AT-1 defect impairs this process. However, ceruloplasmin is not listed in the mammalian "acetylome."[19] To experimentally assess whether AT-1 deficiency might affect ceruloplasmin secretion, we reduced AT-1 expression in HepG2 cells with small interfering RNA (siRNA). As a result, 30% less ceruloplasmin was secreted, consistent with the hypothesis that AT-1 deficiency can indeed reduce ceruloplasmin levels.

Is AT-1 deficiency a copper metabolism disorder? Treatment with copper in three of the patients did not result in an increase in copper or ceruloplasmin levels in serum. Clinically it was reported that the treatment did not change the condition in two patients and resulted in an improvement in one patient who nevertheless died at age 4 years. The brain abnormalities we documented (cortical and cerebellar hypoplasia and hypomyelination; Figure 2) are also reported in patients with Menkes disease.[8] It seems possible that ATP7A, which is normally glycosylated, also undergoes acetylation.[21,22] At least six other ATPases are acetylated.[19] However, the patients we report with AT-1 deficiency did not show other signs of

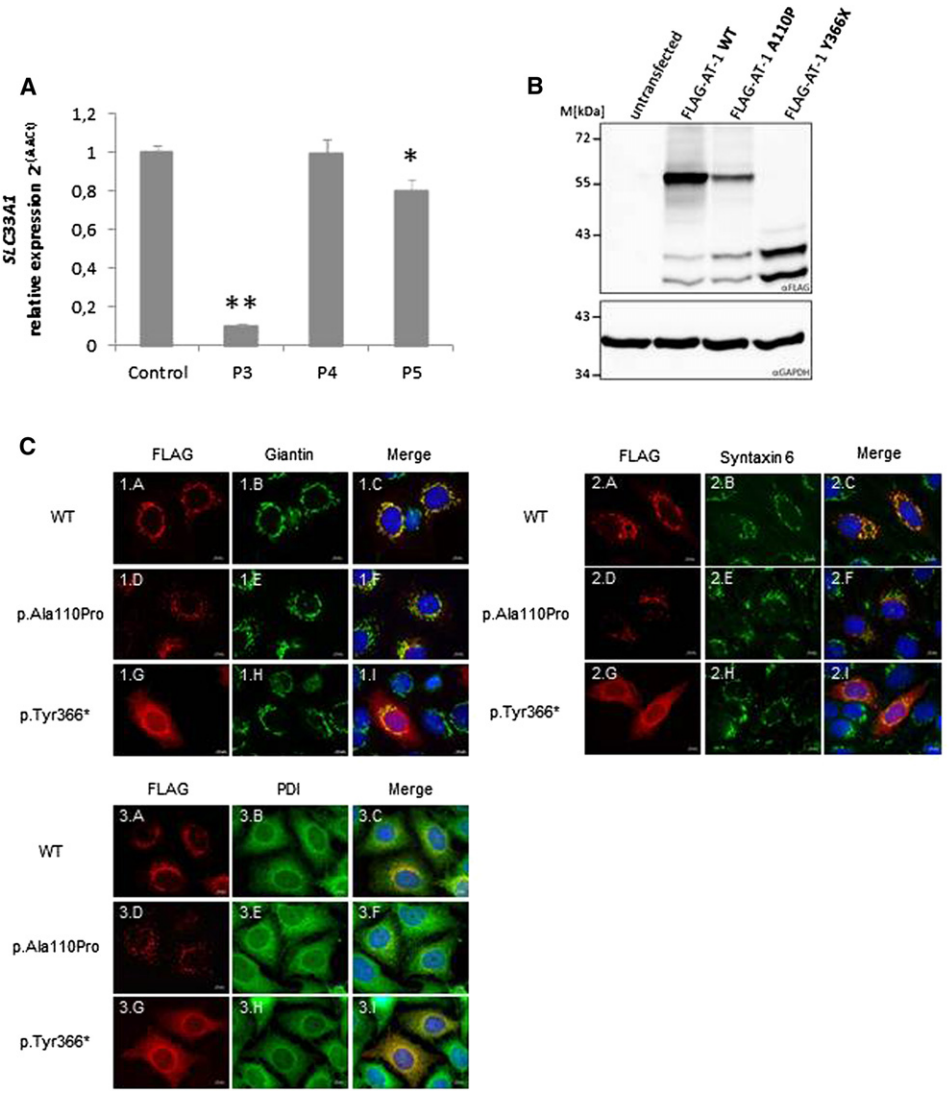

Figure 4. Consequences of the Mutations

(A) Quantitative real-time PCR analyses revealing unchanged (P4 = patient 4) and significantly reduced (P3 = patient 3 and P5 = patient 5) *SLC33A1* expression in patient fibroblasts compared to a normal control cell line. Statistical analysis was done by an unpaired Student's t test compared to wild-type expression in control cells. Errors are given as SEM. The p values (*$p < 0.0001$; **$p = 0.0040$) were adjusted according to Bonferroni.

(B) Western blot analysis of cell extracts (30 μg) from transiently transfected MCF-7 cells expressing the wild-type and mutated forms of AT-1. The blot was probed with a mouse monoclonal FLAG antibody. Untransfected cells and the housekeeping gene *GAPDH* were used as controls.

(C) Subcellular localization of wild-type and mutated AT-1. The proteins were visualized by indirect immunofluorescent analysis of MCF-7 cells transiently transfected with different FLAG-AT-1 expression constructs (red). The cells were fixed, permeabilized, and incubated with the monoclonal antibody raised against the FLAG epitope. The wild-type AT-1 protein shows a perinuclear cytoplasmic localization, where it colocalizes with the Golgi marker proteins Giantin and Syntaxin 6 (green, 1.A–1.C and 2.A–2.C). The protein carrying the missense mutation Ala110Pro produced a punctate pattern and localized neither with the Golgi nor with the ER (PDI, 1.D–1.F, 2.D–2.F, 3.D–3.F). The 184-amino-acid-long truncated AT-1 protein mimicking the nonsense mutation Tyr366* was found in the cytoplasm, where the staining pattern coincided with the ER marker PDI (3.G–3.I). The nuclei were counterstained with DAPI and scale bars represent 10 μm.

profound body copper deficiency, such as typical brittle hair, hypopigmentation, and connective tissue laxity as seen in Menkes disease that would be expected with reduced ATP7A-mediated metallation of copper enzymes.[8] It seems conceivable that acetylation of ATP7A may be required for copper absorption and delivery to the CNS, but not for metallation of copper enzymes. There are also no signs of copper toxicity as in Wilson disease with hepatic cirrhosis and basal ganglia degeneration. T2* sequences available from two patients did not show signs of iron or copper accumulation (images not shown). Moreover, copper analyses in various organs performed in a subset of our patients showed normal values, indicating that the defect in AT-1 may lead to very low ceruloplasmin

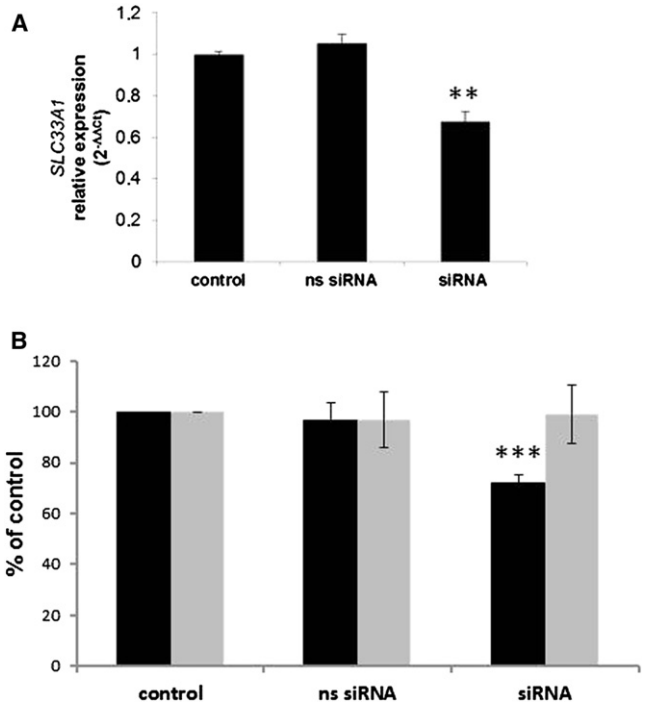

Figure 5. Downregulation of AT-1 Reduces Ceruloplasmin Secretion in HepG2 Cells

(A) Quantitative real-time PCR analysis revealing unchanged (ns siRNA) and statistically significant reduced (siRNA) *SLC33A1* expression in HepG2 cells 2 days after transfection with and without siRNA (control).

(B) Densitometric quantification of three independent western blot experiments. 30 μl medium of the equal number of HepG2 cells were analyzed 2 days after transfection with *SLC33A1*-specific siRNA (control). Compared to cells transfected without siRNA (control) or nonsilencing siRNA (ns siRNA) Ceruloplasmin (black bars), secretion was ~30% reduced but albumin (gray bars) secretion unaltered in cells transfected with *SLC33A1*-specific siRNA (siRNA).

Statistical analysis was done by an unpaired Student's t test compared to wild-type expression in control cells. Errors are given as SEM. The p values were adjusted according to Bonferroni (**$p < 0.0001$, ***$p = 0.0001$).

but not total body copper deficiency or toxicity. It is therefore likely that the copper levels in serum are low in patients with AT-1 defects on the basis of low ceruloplasmin as in aceruloplasminemia. Aceruloplasminemia patients, however, do not become symptomatic before adulthood and the typical symptoms (anemia, insulin-dependent diabetes mellitus, dementia, and dystonia) do not overlap with the symptoms seen in the patients described here. It has already been shown that deficiency in AT-1 has dramatic effects. Downregulation of AT-1 in human neuroglia cells caused ER expansion as well as autophagic cell death, and knockdown of *Slc33a1* in zebrafish resulted in curved shaped tails and defective axon outgrowth from the spinal cord.[13,18] Taken together, the data available to date indicate that low plasma copper and ceruloplasmin are the diagnostic hallmarks of AT-1 defects but disturbances in copper metabolism may play only a minor role in the pathophysiology. Thus, further investigation of AT-1 function is necessary to understand the role of AT-1 in brain metabolism and function and for developing treatment approaches to prevent neurodegeneration and premature mortality in AT-1-deficient patients.

In conclusion we present a novel childhood neurodegenerative disorder caused by mutations in *SLC33A1*. Low copper and ceruloplasmin in serum in combination with congenital cataracts and hearing loss seem to be the diagnostic hallmarks but the phenotypic spectrum remains to be explored. For further dissection of the clinical and biochemical effects of defective acetylation in brain development and function, generation and investigation of AT-1-deficient cell and animal models is necessary.

Supplemental Data

Supplemental Data include Supplemental Experimental Procedures, five figures, and one table and can be found with this article online at http://www.cell.com/AJHG/.

Acknowledgments

We thank Ines Müller and Melanie Bienek for excellent technical assistance. Part of this work was financed by the European Union's Seventh Framework Program under grant agreement number 241995, project GENCODYS, the Intramural Research Program of the National Institutes of Health, Bethesda, MD (Project #HD008768-08), and the German Research Foundation (GA 354/9-1).

Received: September 20, 2011
Revised: October 20, 2011
Accepted: November 30, 2011
Published online: January 12, 2012

Web Resources

The URLs for data presented herein are as follows:

Online Mendelian Inheritance in Man (OMIM), http://www.omim.org

SOSUI program, http://bp.nuap.nagoya-u.ac.jp/sosui/

References

1. Kim, B.E., Nevitt, T., and Thiele, D.J. (2008). Mechanisms for copper acquisition, distribution and regulation. Nat. Chem. Biol. *4*, 176–185.
2. Rae, T.D., Schmidt, P.J., Pufahl, R.A., Culotta, V.C., and O'Halloran, T.V. (1999). Undetectable intracellular free copper: the requirement of a copper chaperone for superoxide dismutase. Science *284*, 805–808.
3. de Bie, P., Muller, P., Wijmenga, C., and Klomp, L.W. (2007). Molecular pathogenesis of Wilson and Menkes disease: correlation of mutations with molecular defects and disease phenotypes. J. Med. Genet. *44*, 673–688.
4. Ferenci, P. (2004). Pathophysiology and clinical features of Wilson disease. Metab. Brain Dis. *19*, 229–239.

5. Harris, Z.L., Takahashi, Y., Miyajima, H., Serizawa, M., MacGillivray, R.T., and Gitlin, J.D. (1995). Aceruloplasminemia: molecular characterization of this disorder of iron metabolism. Proc. Natl. Acad. Sci. USA *92*, 2539–2543.
6. Chelly, J., Tümer, Z., Tønnesen, T., Petterson, A., Ishikawa-Brush, Y., Tommerup, N., Horn, N., and Monaco, A.P. (1993). Isolation of a candidate gene for Menkes disease that encodes a potential heavy metal binding protein. Nat. Genet. *3*, 14–19.
7. Vulpe, C., Levinson, B., Whitney, S., Packman, S., and Gitschier, J. (1993). Isolation of a candidate gene for Menkes disease and evidence that it encodes a copper-transporting ATPase. Nat. Genet. *3*, 7–13.
8. Kaler, S.G. (2011). ATP7A-related copper transport diseases-emerging concepts and future trends. Nat Rev Neurol *7*, 15–29.
9. Horváth, R., Freisinger, P., Rubio, R., Merl, T., Bax, R., Mayr, J.A., Shawan, Müller-Höcker, J., Pongratz, D., Moller, L.B., et al. (2005). Congenital cataract, muscular hypotonia, developmental delay and sensorineural hearing loss associated with a defect in copper metabolism. J. Inherit. Metab. Dis. *28*, 479–492.
10. Borck, G., Ur Rehman, A., Lee, K., Pogoda, H.M., Kakar, N., von Ameln, S., Grillet, N., Hildebrand, M.S., Ahmed, Z.M., Nürnberg, G., et al. (2011). Loss-of-function mutations of ILDR1 cause autosomal-recessive hearing impairment DFNB42. Am. J. Hum. Genet. *88*, 127–137.
11. Miller, S.A., Dykes, D.D., and Polesky, H.F. (1988). A simple salting out procedure for extracting DNA from human nucleated cells. Nucleic Acids Res. *16*, 1215.
12. Kanamori, A., Nakayama, J., Fukuda, M.N., Stallcup, W.B., Sasaki, K., Fukuda, M., and Hirabayashi, Y. (1997). Expression cloning and characterization of a cDNA encoding a novel membrane protein required for the formation of O-acetylated ganglioside: a putative acetyl-CoA transporter. Proc. Natl. Acad. Sci. USA *94*, 2897–2902.
13. Lin, P., Li, J., Liu, Q., Mao, F., Li, J., Qiu, R., Hu, H., Song, Y., Yang, Y., Gao, G., et al. (2008). A missense mutation in SLC33A1, which encodes the acetyl-CoA transporter, causes autosomal-dominant spastic paraplegia (SPG42). Am. J. Hum. Genet. *83*, 752–759.
14. Schlipf, N.A., Beetz, C., Schüle, R., Stevanin, G., Erichsen, A.K., Forlani, S., Zaros, C., Karle, K., Klebe, S., Klimpe, S., et al. (2010). A total of 220 patients with autosomal dominant spastic paraplegia do not display mutations in the SLC33A1 gene (SPG42). Eur. J. Hum. Genet. *18*, 1065–1067.
15. Hattori, A., Sasaki, M., Sakuma, H., Saito, Y., Komaki, H., Nakagawa, E., and Sugai, K. (2010). [Hereditary spastic paraplegia associated with congenital cataracts, mental retardation and peripheral neuropathy]. No To Hattatsu *42*, 454–457.
16. Hirabayashi, H., Takahashi, W., Shinohara, N., Hata, T., and Shinohara, Y. (1998). [Complicated form of spastic paraplegia with congenital cataract: a case report]. Rinsho Shinkeigaku *38*, 38–41.
17. Miyama, S., Arimoto, K., Kimiya, S., and Tomi, H. (2000). Complicated hereditary spastic paraplegia with peripheral neuropathy, optic atrophy and mental retardation. Neuropediatrics *31*, 214–217.
18. Jonas, M.C., Pehar, M., and Puglielli, L. (2010). AT-1 is the ER membrane acetyl-CoA transporter and is essential for cell viability. J. Cell Sci. *123*, 3378–3388.
19. Choudhary, C., Kumar, C., Gnad, F., Nielsen, M.L., Rehman, M., Walther, T.C., Olsen, J.V., and Mann, M. (2009). Lysine acetylation targets protein complexes and co-regulates major cellular functions. Science *325*, 834–840.
20. Ko, M.H., and Puglielli, L. (2009). Two endoplasmic reticulum (ER)/ER Golgi intermediate compartment-based lysine acetyltransferases post-translationally regulate BACE1 levels. J. Biol. Chem. *284*, 2482–2492.
21. Kim, B.E., and Petris, M.J. (2007). Phenotypic diversity of Menkes disease in mottled mice is associated with defects in localisation and trafficking of the ATP7A protein. J. Med. Genet. *44*, 641–646.
22. Liu, Y., Pilankatta, R., Hatori, Y., Lewis, D., and Inesi, G. (2010). Comparative features of copper ATPases ATP7A and ATP7B heterologously expressed in COS-1 cells. Biochemistry *49*, 10006–10012.